Draft version May 21, 2010
Preprint typeset using LaTeX style emulateapj v. 02/07/07

M31 PIXEL LENSING EVENT OAB-N2: A STUDY OF THE LENS PROPER MOTION

S. Calchi Novati[1,2,3], M. Dall'Ora[4], A. Gould[5], V. Bozza[1,2,3], I. Bruni[6], F. De Paolis[7], M. Dominik[8*], R. Gualandi[6], G. Ingrosso[7], Ph. Jetzer[9], L. Mancini[1,2,3,10], A. Nucita[11], G. Scarpetta[1,2,3], M. Sereno[12,13], F. Strafella[7] (PLAN collaboration[†])

[1] Dipartimento di Fisica "E. R. Caianiello", Università di Salerno, Via Ponte Don Melillo, 84084 Fisciano (SA), Italy
[2] INFN, sezione di Napoli, Italy
[3] Istituto Internazionale per gli Alti Studi Scientifici (IIASS), Vietri Sul Mare (SA), Italy
[4] INAF-OAC, Italy
[5] Department of Astronomy, Ohio State University, 140 West 18th Avenue, Columbus, OH 43210, US
[6] INAF-OAB, Italy
[7] Dipartimento di Fisica, Università del Salento and INFN, Sezione di Lecce, CP 193, 73100 Lecce, Italy
[8] SUPA, University of St Andrews, School of Physics & Astronomy, North Haugh, St Andrews, KY16 9SS, United Kingdom
[9] Institute for Theoretical Physics, University of Zürich, Winterthurerstrasse 190, 8057 Zürich, Switzerland
[10] Dipartimento di Ingegneria, Università del Sannio, Corso Garibaldi 107, 82100 Benevento, Italy
[11] XMM-Newton Science Operations Centre, ESAC, ESA, PO Box 78, 28691 Villanueva de la Cañada, Madrid, Spain
[12] Dipartimento di Fisica, Politecnico di Torino, Corso Duca degli Abruzzi 24, 10129 Torino, Italia and
[13] INFN, Sezione di Torino, 10125, Torino, Italia

Draft version May 21, 2010

ABSTRACT

We present an updated analysis of the M31 pixel lensing candidate event OAB-N2 previously reported in Calchi Novati et al. (2009a). Here we take advantage of new data both astrometric and photometric. Astrometry: using archival 4m-KPNO and HST/WFPC2 data we perform a detailed analysis on the event source whose result, although not fully conclusive on the source magnitude determination, is confirmed by the following light curve photometry analysis. Photometry: first, unpublished WeCAPP data allows us to confirm OAB-N2, previously reported only as a viable candidate, as a well constrained pixel lensing event. Second, this photometry enables a detailed analysis in the event parameter space including the effects due to finite source size. The combined results of these analyses allow us to put a strong lower limit on the lens proper motion. This outcome favors the MACHO lensing hypothesis over self lensing for this individual event and points the way toward distinguishing between the MACHO and self-lensing hypotheses from larger data sets.

Subject headings: dark matter — gravitational lensing — galaxies: halos — galaxies: individual (M31, NGC 224) — Galaxy: halo

1. INTRODUCTION

Gravitational microlensing is an established tool of research. The original motivation (Paczyński 1986) has been the search for dark matter in the form of massive compact halo objects (MACHOs) (for a recent discussion from a larger point of view on dark matter and gravitational lensing we refer to Massey et al. 2010). The first lines of sight explored to this purpose have been those toward the Magellanic Clouds (LMC and SMC). Microlensing campaigns toward the Galactic center have then been used to constrain Galactic structure (Moniez 2010 and references therein) and, more recently, for the detection of extra-solar planets (Gaudi 2010; Dominik 2010 and references therein).

Results on MACHOs toward the LMC and the SMC have been reported by the MACHO (Alcock et al. 2000), the EROS (Tisserand et al. 2007) and the OGLE collaboration (Wyrzykowski et al. 2009). There is agreement that MACHOs are excluded as a major component of dark matter for a wide range of possible mass values (down to about 10^{-6} $M_\odot$). There remains however a range, $(0.1 - 1)$ $M_\odot$, in which the results of the MACHO collaboration, as confirmed by Bennett (2005), indicate that MACHOs might compose about a $f = 20\%$ fraction of the Milky Way (hereafter MW) halo mass at least up to the distance of the LMC. This outcome is challenged by the results of the EROS and the OGLE collaborations. A possible contamination of the microlensing signal due to MACHOs, once the background of intrinsic variable stars that can mimic microlensing is excluded, is *self lensing*, wherein both the source and lens belong to some luminous population[1]. (This possibility has been first considered in Sahu 1994; Gould 1995 and further studied by several authors, e. g. Gyuk et al. 2000; Mancini et al. 2004; we refer also to Calchi Novati et al. 2009b for a specific analysis of the OGLE-II results, to Calchi Novati et al. 2006 for a study of the possible contribution of the LMC own dark matter halo to the observed MACHO events and to Moniez 2010 for an updated review on this issue). Indeed, the fact that the only remaining allowed mass range for MACHOs, from the LMC analyses, corresponds to that of the stars that might also act as lenses may be indicative of some observational bias (we recall that the characteristics of the microlensing events, in particular their duration, depend on the lens

[*] Royal Society University Research Fellow
[†] http://plan.physics.unisa.it/index.htm
[1] Hereafter we will refer to "self lensing", broadly speaking, for any microlensing event with a *stellar* lens, not necessarily belonging to the *same* stellar population of the source.

mass). On the other hand, if the reported events are really to be attributed to MACHOs, a fortiori for such a sizeable fraction as that implied by the MACHO collaboration results, this might have some deeper astrophysical meaning.

Beyond the Magellanic Clouds, the next suitable target for a microlensing search is our nearby and similar galaxy of Andromeda, M31 (Crotts 1992; Baillon et al. 1993; Jetzer 1994). It allows one to explore a different line of sight through the MW halo; we can fully map M31's own dark matter halo (which is not possible for the MW, this being perhaps the most severe limitation of LMC studies); finally, the inclination of M31 is expected to give rise to a characteristic signature in the spatial distribution of M31 halo events, so facilitating their identification against the contamination of self-lensing events. Because of the distance of M31, the sources for microlensing events are no longer resolved objects, at least for ground-based telescopes, so that we enter the *pixel lensing* regime (Gould 1996). Several observational campaigns have already been undertaken along this line of sight (for a review we refer to Calchi Novati 2009). The results obtained up to now on the MACHO issue are controversial. The POINT-AGAPE collaboration claimed evidence of a MACHO signal in the same mass range indicated by the MACHO LMC analysis (Calchi Novati et al. 2005). This outcome, however, has been challenged by the MEGA collaboration who concluded that the detected signal is compatible with the expected self-lensing rate (de Jong et al. 2006). Finally, the WeCAPP collaboration is expected to present the final analysis of their 11-year campaign[2].

The issue of self lensing for M31 microlensing is even more difficult than for the LMC for two principal reasons. First, the expected self-lensing rate is quite large with respect to MACHO lensing, at least in the inner part of M31 (in which both signals have the larger expected rate because of the huge number of available sources). The exact ratio depends not only on the unknown halo fraction in the form of MACHOs and on the MACHO mass but also on the not fully understood contribution of M31 *stellar* lensing. (In fact, a possible approach to deal with this problem is that followed in the already cited analyses of Calchi Novati et al. 2005 and de Jong et al. 2006, where statistical arguments were used for a full set of events. Interestingly, a main point of disagreement between these two analyses is the role played by self lensing with respect to MACHO lensing, as discussed also in Ingrosso et al. 2006, 2007). Second, the lack of knowledge of the source flux, specific for the "pixel" lensing regime, adds a further degeneracy in the event parameter space that makes the disentangling of the two signals more difficult. In particular, this degeneracy implies that, rather than determining the Einstein time, $t_{\rm E}$, the impact parameter, u_0, and the source flux ϕ^*, from the light curve one can usually reliably estimate only the full-width-half-maximum duration, $t_{\rm FWHM} = t_{\rm E}\, f(u_0)$ (Gondolo 1999), and the flux deviation at maximum amplification, $\Delta\phi = \phi^*\, A_{\rm max}(u_0)$, usually expressed in term of magnitude, e. g. ΔR (Gould 1996; Wozniak & Paczynski 1997).

This problem of interpretation of the lens nature, together with the overall small number of *reliable* microlensing candidate events reported toward M31 so far, make the issue of a correct astrophysical understanding of *single* events that may contain precious additional information particularly relevant. For M31 lensing this issue has been first emphasized by the WeCAPP collaboration in Riffeser et al. (2006). The WeCAPP collaboration, furthermore, presented an extremely detailed analysis of the microlensing event PA-S3/GL1 (first reported by POINT-AGAPE, Paulin-Henriksson et al. 2003; Belokurov et al. 2005, and subsequently, Riffeser et al. 2003, detected in their own data set by the WeCAPP collaboration itself). Also thanks to the excellent sampling along the bump assured by the two independent data sets, and on the basis of a study of the *source finite size effect* (Witt & Mao 1994), Riffeser et al. (2008) showed that this extremely bright microlensing event is more likely to be attributed to MACHO lensing than to self lensing. Interestingly, this would hold even though the event is located very near to the M31 center, $d \sim 4'$, where the expected self-lensing rate is larger.

In fact, the first detailed analysis of a M31 pixel lensing event aimed at the characterization of the lens nature has been presented by the POINT-AGAPE collaboration for the event PA-N1 (Aurière et al. 2001). With the source magnitude and color fixed thanks to an analysis of archival *Hubble Space Telescope* (HST) data, and based on a specific Monte Carlo simulation of the experiment, where the observed characteristics of the event had been used to delimit the possible parameter space (using in particular a lower limit for the lens proper motion), Aurière et al. (2001) conclude that the PA-N1 lens is more likely a MACHO if the mass halo fraction in the form of compact halo object is above 20%. The results of this analysis have been however challenged by the MEGA collaboration (who also reported this event as MEGA-ML16, de Jong et al. 2006), in particular by Cseresnjes et al. (2005) who argued, on the basis of new HST observations, against the source identification reported in Aurière et al. (2001).

Following the strong interest in the characterization of single events, in the present work we will present an updated analysis of the microlensing candidate event OAB-N2 first reported by the PLAN (Pixel Lensing ANdromeda) collaboration in Calchi Novati et al. (2009a). First, we present a new analysis related to the issue of the source identification and characterization using KPNO and HST archival images, Sect. 2.1. The driving motivation for a new analysis comes from the significantly improved sampling along the flux deviation due to the access to unpublished data of the WeCAPP collaboration (Riffeser et al. 2001). As we show, these new data allow us to firmly establish the microlensing nature of this flux variation and to carry out an improved and more detailed analysis of the lensing parameter space with the inclusion of the finite source size effect. This allows us to put some constraints on the relative lens-source *proper motion* (Gould 1994), Sect. 2.2. In Sect. 3 we discuss the outcomes of the analysis within the framework of the Monte Carlo simulation of our M31 pixel lensing experiment. The limits on the lens proper motion are here relevant as they can be used as a tool to distinguish bewteen the self lensing and MACHO lensing nature of this microlensing event.

[2] A. Riffeser and S. Seitz, private communication.

2. ANALYSIS

2.1. *Source identification and characterization*

In Calchi Novati et al. (2009a) we have tentatively identified the OAB-N2 candidate event source with a rather bright star, $R = 20.9$ $R - I = 1.2$, the nearest Massey et al. (2006) catalog object to our estimated event position. Also motivated by the updated light curve analysis that suggests a fainter source star (Sect. 2.2) we have performed a more detailed analysis. As a result we find this catalog star *not to be* the event source. However, the available data do not allow us to conclusively identify and characterize the candidate event source.

More specifically, we have proceeded as follows. We have downloaded the images used by Massey et al. (2006) for their analysis, collected at the 4m Mayall-KPNO telescope[3]. In particular we have used the I band image M31F5I-1.fits with exposure time of 150 sec. We have selected a sample of $\sim$ 200 stars brighter than $R_C = 20$ identified both on M31F5I-1 and our OAB image to carry out a pixel-to-pixel relative astrometry calibration[4], for which we get to rms $\sim 0.2''$. Because at maximum amplification the event is a resolved object, the accuracy of the event position determination is better, below $0.1''$. Taking therefore $\sigma = 0.2''$ we find that the catalog star previously identified as the event source is in fact about 4.3σ away from the event position (and this is also confirmed to be the star reported in the catalog nearest to the event position), whereas a fainter object, not present in the catalog but still clearly visible (as checked also on a few other Massey et al. 2006 images), is located at only 1.3σ (hereafter we refer to the catalog object as S1 and to the fainter one as S2). This result is confirmed by an independent analysis in which both the KPNO and the OAB images are first "astrometrised" with respect to the USNO-B1 catalog (Monet et al. 2003). This analysis, however, has worse precision since the nearest catalog objects that avoids the inner M31 central region are located at about $3' - 4'$ from the event position.

As a second step we perform PSF photometry analysis of the KPNO I-band image. For S2 we estimate $I_C = 20.5 \pm 0.2$. As expected, this is fainter than S1, by about $\sim$ 1 mag, but the statistical error turns out to be extremely large, more than twice greater than the average error we find for stars of similar brightness in this image. Furthermore, we find also the output fit *sharpness* parameter for S2 to be a clear outlier. Both these elements indicate that S2 is more likely to be a *blend* of two or more stars.

To investigate further this issue we have looked for archival HST images of this field. We find 2 F606W and 3 F814W WFPC2/WF3 images (pixel scale $0.1''$) available (GO 5971, P.I. Griffiths), out of which, however, only a 1000 sec exposure time F814W image is reported not to have quality problems, which we then use for our analysis. The cross-match of the KPNO image with the HST one is carried out by the identification of 12 stars on both images and we end up with a relative astrometry precision of rms $\sim 0.1''$. Corresponding to the KPNO S2 position we find two stars (as identified also in the HST photometry analysis) lying within a distance of about $0.3''$ (corresponding roughly to one KPNO pixel). This confirms our previous conclusion on S2 being a blend. Both of these stars lie within 3σ of the estimated event position, with the brighter one lying nearer (about 1σ). Finally, we have performed a photometry analysis on the HST image. In particular we have made use of both the HST Stetson[5] PSF and of the HSTphot WFPC2 photometry package (Dolphin 2000), for which we have considered three options for the background fit and PSF evaluation. In accord with this latter analysis we find, for the brighter of the two sources lying at the S2 position, $I_{\rm instr} \sim 20.6 - 21.1$[6], depending on the photometry option, with a formal statistical error $\sigma \sim$ 0.1 mag, and a magnitude difference between the two sources of $\sim$ 0.2 mag. For the first analysis we find a somewhat brighter magnitude value for the brighter object, although with larger error, $\sigma \sim 0.2 - 0.3$ mag, and larger magnitude difference, $\sim$ 0.8 mag. Taking the HSTphot analysis as the fiducial one, we get to a final estimate of $I_{\rm instr} = 20.8 \pm 0.3$ for the brighter star. The lack of color information, the large M31 background level and crowdedness at the event position which makes the photometry less reliable, and the presence of a second, fainter, star as a viable source do not allow us to consider these results on the HST photometry as conclusive.

Overall, this new astrometry and *image*-based photometry analysis, although with the already stressed caveats, allows us to definitively affirm that the OAB-N2 source is a fainter star than previously concluded. This result turns out to be in agreement with the outcome of the new photometry *light curve*-based analysis that we will detail in the following Section.

2.2. *Light curve analysis*

The microlensing flux variation OAB-N2 has been first reported in Calchi Novati et al. (2009a) in the framework of a long-term pixel lensing monitoring of M31 by the PLAN collaboration at the 152cm Loiano telescope (Calchi Novati et al. 2007). This appears as a bright, $\Delta R \sim 19$, short duration, $t_{\rm FWHM} \sim 3$ days, flux variation, lying at about $3'$ from the M31 center, with a flat baseline on both previous OAB and POINT-AGAPE data sets. These characteristics, the excellent agreement with a Paczyński shape together with the rather red color, $R - I \sim 1.1$ (this feature is against the alternative hypothesis of contamination from some kind of eruptive variable, usually bluer), have all been considered as strong indications of the genuine microlensing origin of this flux variation. However, the analysis presented in Calchi Novati et al. (2009a) suffered from the serious limitation in that data points were available on the rising part of the flux variation only. This did not allow us to test the expected symmetric shape characteristic of

[3] http://archive.noao.edu.
[4] The KPNO and OAB images have pixel scales of $0.26''$ and $0.58''$, respectively.
[5] P. Stetson, private communication.
[6] We recall that the F814W filter is similar to the standard Cousin-I.

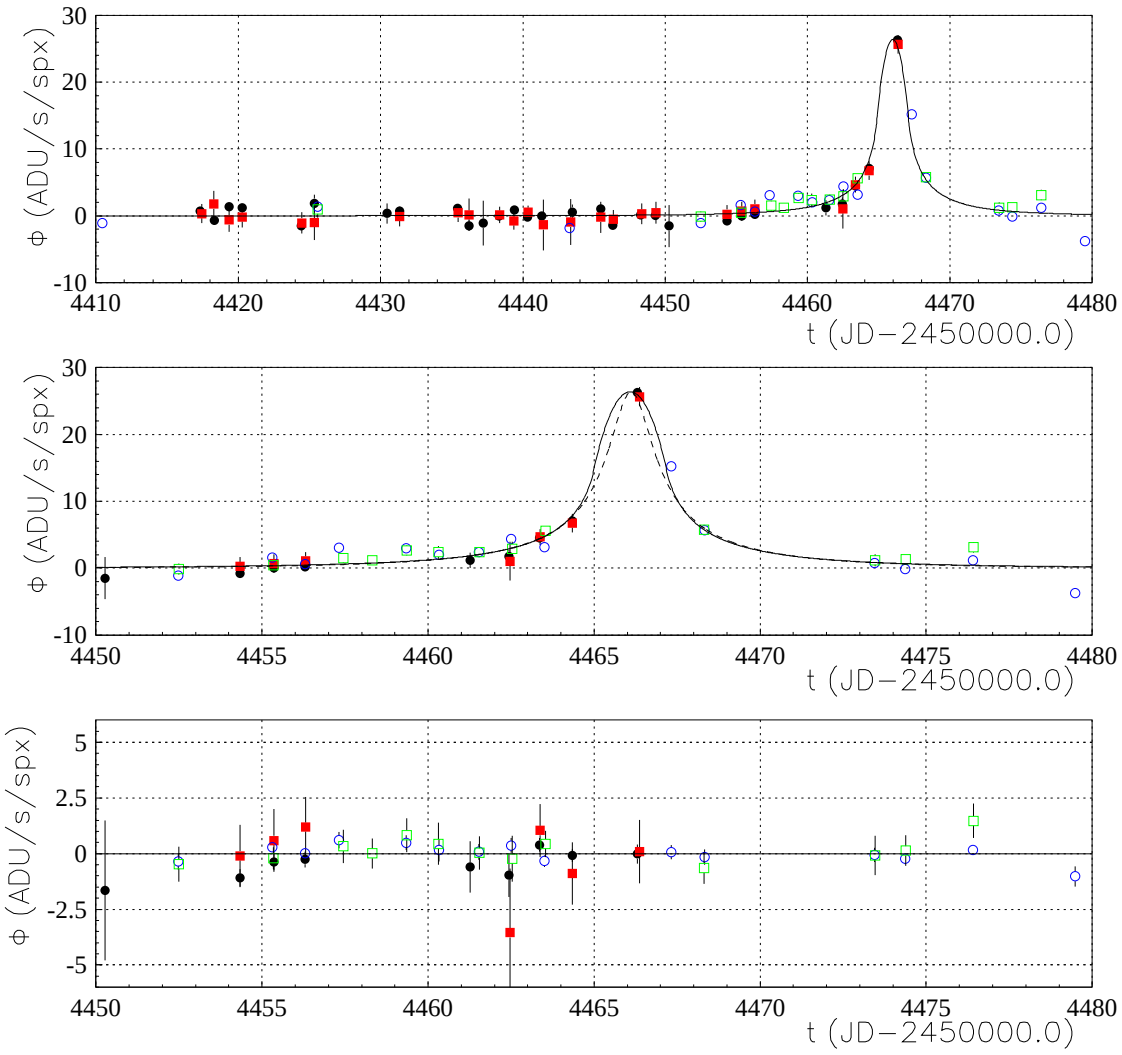

FIG. 1.— OAB-N2 light curve and residuals with respect to the best fit. Circles (boxes) are for R (I)-band, with filled (empty) symbols for OAB (WeCAPP) data. Top and middle panels: the solid (dashed) lines show the best fit with (without) inclusion of finite size source effect. The abscissa units are time in days (JD-2450000.0). The ordinate units are flux in ADU s^{-1} per superpixel.

TABLE 1
OAB-N2 : CHARACTERISTICS AND PACZYŃSKI FIT RESULTS (CORRECTED FOR FINITE SOURCE SIZE AND LIMB DARKENING EFFECTS)

α	δ	χ^2	t_0 (JD-2450000.0)	u_0	ρ	$t_{\rm E}$ (days)	t_*	R_*	$R-I$
$0^{\rm h}42^{\rm m}50^{\rm s}.31$	$41°18'40''.1$	326.16	$4466.23^{+0.13}_{-0.10}$	$0.07^{+0.07}$	$0.154^{+0.062}_{-0.043}$	$8.1^{+2.7}_{-2.1}$	$1.245^{+0.10}_{-0.13}$	22.25 ± 0.51	1.24 ± 0.03

NOTE. — It results $\chi^2/{\rm dof} = 1.24$. The reported error are for $\Delta\chi^2 = 1.0$ (68.3% level). For the impact parameter u_0 there is no minimum value at the requested confidence level (as shown also in Fig. 2). For the (normalized) angular radius ρ we find also a secondary minimum at $\rho \sim 0.08$ (correspondingly $u_0 \sim 0.11$ and $t_* \sim 0.55$). The source magnitude and color values are *not* corrected for extinction.

microlensing events and to definitively conclude on the microlensing nature of this flux variation. We are now able to overcome this problem as data points along the descent of the bump have been made available to us from the WeCAPP collaboration (Riffeser et al. 2001). These data have been collected at the 0.8 m Wendelstein telescope in two pass bands, R and I, similar to those used for OAB data.

The analysis of the joint OAB-WeCAPP light curve, shown in Fig. 1 together with the results of the fit to be discussed below, is extremely interesting. WeCAPP data alone, missing the peak of the flux variation, do not allow to detect this flux variation. They are however essential to constrain the flux variation as they nicely cover the descent and contribute to the already excellent coverage along the rising wing of the flux variation, extremely important to robustly constrain the microlensing parameters (Baltz & Silk 2000; Dominik 2009). The excellent agreement with

a Paczyński shape and the achromaticity are now probed along all of the flux variation. *We confirm the genuine microlensing nature of OAB-N2.* This conclusion is enhanced by the fact that we are considering two completely independent data sets analyzed, moreover, following two different schemes of photometry reduction, the "superpixel" photometry with empirical correction of seeing variations for OAB data (Ansari et al. 1997; Calchi Novati et al. 2002) and difference image analysis for WeCAPP data (Alard & Lupton 1998; Gössl & Riffeser 2002). For a recent analysis on difference imaging photometry specific for high surface brightness targets such as the M31 bulge region we refer to Kerins et al. (2010).

The excellent sampling along the bump allows us to move further in the analysis and to look for a better characterization of this microlensing event. In particular we want to look for signatures of *finite source* effect (Witt & Mao 1994) with the purpose to eventually constrain the lens *proper motion* (Gould 1994).

The relevant parameter for the finite source effect is $\rho \equiv \theta_*/\theta_{\rm E}$, where θ_* is the angular radius of the source and $\theta_{\rm E}$ the angular Einstein radius. We recall that finite source effects become relevant whenever ρ gets larger than the impact parameter u. For the event amplification, following the scheme outlined in Yoo et al. (2004), we write

$$A\left(t\right) = -A_{\rm pacz}\left(t\right) B_1\left(z\right) \Gamma_\lambda + A_{\rm fs}\,. \tag{1}$$

Here $A_{\rm pacz}$ is the standard Paczyński amplification, $A_{\rm fs}$ is the amplification including the finite source effect, for which we use the exact Witt & Mao (1994) expression (for a different approach we refer to the recent analysis in Lee et al. 2009), $z \equiv u/\rho$, and Γ_λ are the, wavelength dependent, linear limb darkening coefficients. The expression for $B_1(z)$ is given in Eq. 16 of Yoo et al. (2004).

The inclusion of limb darkening is relevant as we know the source flux not to be uniformly distributed across the star surface. To evaluate the Γ_λ we make use of the results of van Hamme (1993). Starting from the event color (the driving and essential parameter) we have to further specify the star temperature, surface gravity and metalicity[7]. To this purpose we make use of the Marigo et al. (2008) isochrones. We consider two cases: a 12 Gyr population with $Z = 0.030$, typical for the bulge, and a 2 Gyr population with $Z = Z_\odot = 0.019$, typical for the disk (Riffeser et al. 2006). From the light curve analysis, and the magnitude zero point, we estimate a dereddened color $(R-I)_C = 1.24$. Taking into account the MW foreground extinction, $E(B-V) = 0.062$ (Schlegel et al. 1998), we get $(R-I)_{0,C} = 1.20$. For bulge/disc sources we then get $T_{\rm eff} \sim 3600/3550$ K, $\log(g) \sim 0.90/0.60$. Finally we get $\Gamma = 0.81/0.81\,(0.62/0.60)$ for R_C (I_C), respectively. Even if we include a term of internal extinction (Riffeser et al. 2006) the final result does not change significantly. Using ${\rm ext}_R = 0.19$ for the bulge we finally get to $\Gamma = 0.80\,(0.59)$, and with $E(B-V) = 0.22$ for the disc we get to evaluate $\Gamma = 0.76\,(0.58)$. In conclusion, we use $\Gamma_\lambda = 0.80, 0.60$ for R and I band data. We reach consistent results basing our analysis on the Claret (2000) limb darkening coefficients instead.

We carry out the light curve Paczyński fit (corrected for finite source size and limb darkening effects) using Eq. 1 for the microlensing amplification[8]. For a simultaneous fit of the two joint data sets with two bands each, overall we have 12 independent parameters (4 and 8 to account for geometry and fluxes, respectively). The microlensing amplification parameters: the Einstein time, $t_{\rm E}$, the minimum value of the impact parameter, u_0, the (normalized) source angular radius, ρ and the time at maximum amplification, t_0. The 8 flux parameters are, for both R and I and OAB and WeCAPP data, the background value and the source flux, ϕ_R and ϕ_I.

Our first purpose is to constrain the normalized source angular radius, ρ, or equivalently $t_* \equiv \rho\, t_{\rm E}$, the source radius crossing time (the Einstein time turns out to be better constrained with respect to ρ). Then, since the event source flux and color can be used to estimate the source angular radius, θ_*, to finally constrain μ, the lens proper motion

$$\mu = \frac{\theta_{\rm E}}{t_{\rm E}} = \frac{\theta_*}{t_*}\,. \tag{2}$$

As a tool we make use of a χ^2 analysis in which we scan the parameter space of one (or more) fit parameters while the remaining are left free and determined, at each step of the scan, by the fit[9]. The main results of this χ^2-based analysis, discussed below, are presented in Table 1 and Fig. 2,3.

A first relevant outcome is the excellent agreement with a Paczyński shape reflected in the small value $\chi^2/{\rm dof} = 1.24$. The best fit value for the source magnitude is significantly *fainter* than in our previous Calchi Novati et al. (2009a) analysis, although affected by a very large error. In particular, the result is 1.3 mag fainter (beyond 95% level) than the Massey et al. (2006) catalog source. Furthermore, it is in agreement with the HST-based estimate in Sect. 2.1 (for I-band magnitude 21.0 ± 0.5 to be compared with 20.8 ± 0.3). Both the source magnitude and the Einstein time are rather well constrained within the fit: at 95% level we obtain $R_* = 22.2^{+0.9}_{-1.1}$ and $t_{\rm E} = 8.2^{+6.9}_{-3.9}$, respectively. This is not the case, however, for the normalized angular radius ρ, which is degenerate with the impact parameter u_0 (the impact parameter is in fact unbounded from below even at the 68.3% level) along two different directions (Fig. 2, top panel). Specifically, we find an absolute minimum at $\rho \approx 0.15$ with $u_0 \approx 0.07$ (along the corresponding direction of degeneracy, u_0 goes to zero with $\rho > 0.1$) and then a secondary minimum, with $\Delta\chi^2 \sim 0.9$, with $\rho \approx 0.08$ and $u_0 \approx 0.11$ (here, just above the 68.3% threshold for $\Delta\chi^2 = 1.0$, ρ goes to zero with roughly constant u_0). The former rather large value of

[7] We make use of the relationship $\Gamma = 2u/(3-u)$ to link Γ to the linear limb darkening parameter u (not to be confused with the microlensing impact parameter) given in van Hamme (1993).

[8] We rescale the error bars, by $\sim 10\%$, so to force, along the baseline, $\chi^2/{\rm dof}$ to unity. This only marginally, however, changes the outcome of the analysis.

[9] We use, within the CERNLIB MINUIT package, the minimization tool MIGRAD "a variable-metric method with inexact line search, a stable metric updating scheme, and checks for positive-definiteness" http://wwwasdoc.web.cern.ch/wwwasdoc/minuit/minmain.html.

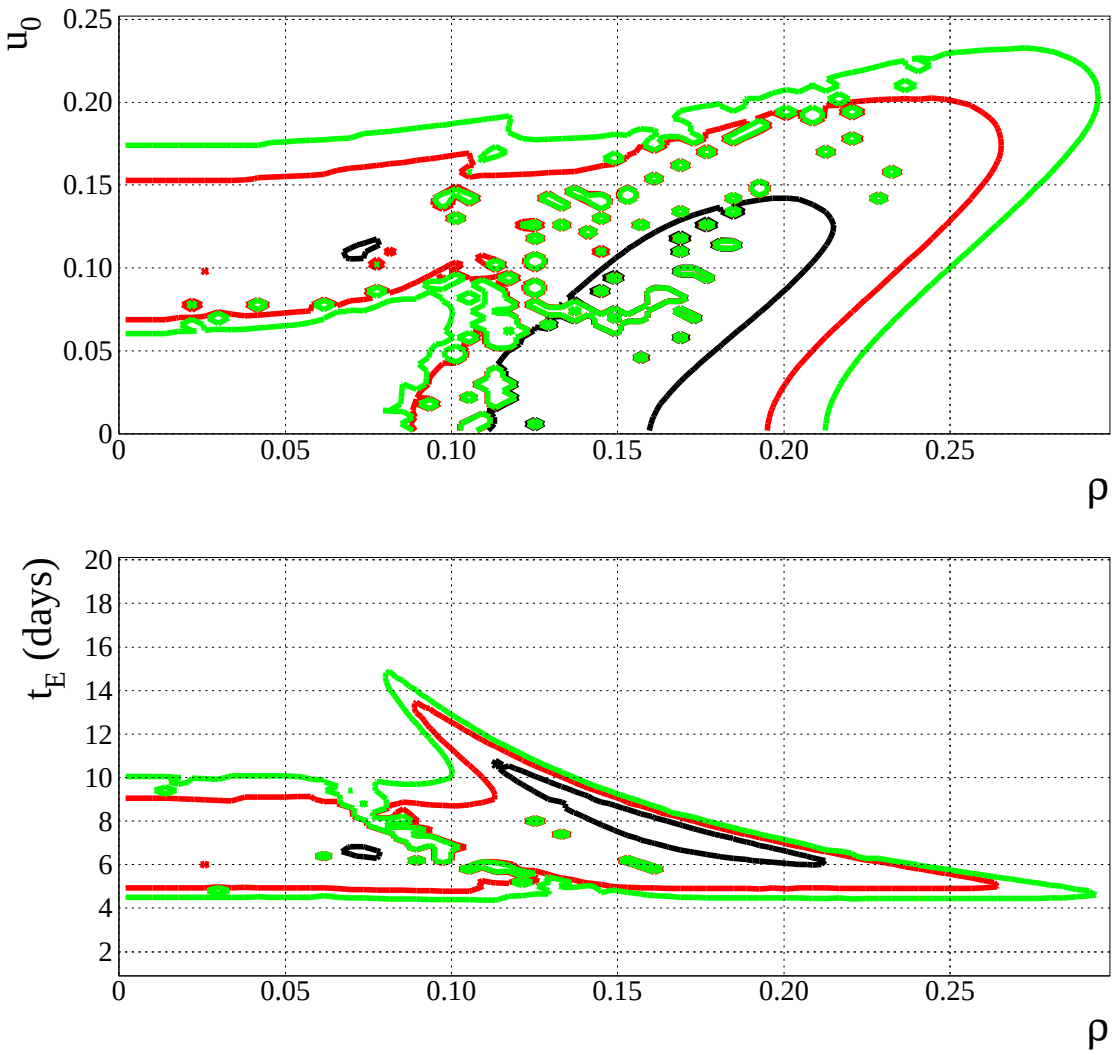

FIG. 2.— 68.3%, 90% and 95% χ^2 contour maps in the parameter space ρ-u_0 (top panel) and ρ-$t_{\rm E}$. ρ, u_0 and $t_{\rm E}$ are the normalized angular radius of the source, the impact parameter and the Einstein time, respectively.

ρ, with $\rho/u_0 \approx 2$ might be taken as an indication of finite size source effect. Given the caveats further addressed below this would make of OAB-N2 the first microlensing event reported toward M31 with a signature of finite size source effect. Indeed, the secondary minimum, as well as the full degenerate parameter space region for $\rho < 0.1$, just above the $\Delta\chi^2 = 1.0$ threshold, do not allow us to draw firm conclusions on this issue. Overall, the indication for $\rho > 0$ remains extremely tenuous. In particular the χ^2 improvement with respect to the case with no inclusion of the finite size parameter, ρ, is only marginal, $\Delta\chi^2 \sim 1$. The inclusion of ρ, however, is essential for the analysis as a tool to allows us to constrain the lens proper motion. The degeneracy for ρ is shown also in the parameter space ρ-$t_{\rm E}$ (Fig. 2, bottom panel). This result is reflected in the estimate of the source radius crossing time for which we find the absolute minimum at $t_* \approx 1.25$ days, but also a secondary minimum at $t_* \approx 0.55$ days (Fig. 3, top panel).

The missing information to get to the lens proper motion μ is the source angular radius, θ_*. To this purpose we use the empirical relationship $\theta_* = \theta_*(V, V-K)$ for *giants* discussed in van Belle (1999). Taking into account the MW foreground extinction (Schlegel et al. 1998), and the Marigo et al. (2008) isochrones as above we estimate, both for a bulge or a disc source, $V = 23.3$ and $V - K = 5.0$. This gives

$$\theta_* = 0.67^{+0.17}_{-0.14} \quad \mu{\rm as}\,, \tag{3}$$

where the error budget is dominated by the statistical uncertainty of the source magnitude within the light curve fit. The result we get to for θ_* is very similar, within 1%, if we additionally take into account the internal M31 bulge or disc extinction as discussed above. In these cases we would find a *fainter* source with a *bluer* color, and these two effects balance one each other in the evaluation of the angular radius. (An alternative, more recent and more accurate $\theta_* = \theta_*(V, V-K)$ relationship is discussed in Kervella et al. 2004. The result we would get to in this case for θ_* is about 20% larger, still comfortably within 1σ. For our discussion we however prefer that discussed in van Belle 1999 as it is derived from a sample of data with $2.0 \leq V - K \leq 8.0$ whereas Kervella et al. 2004 use a more Cepheid-specific sample with $1.0 \leq V - K \leq 2.4$, with the former being more suitable for us given the source color). For the discussion

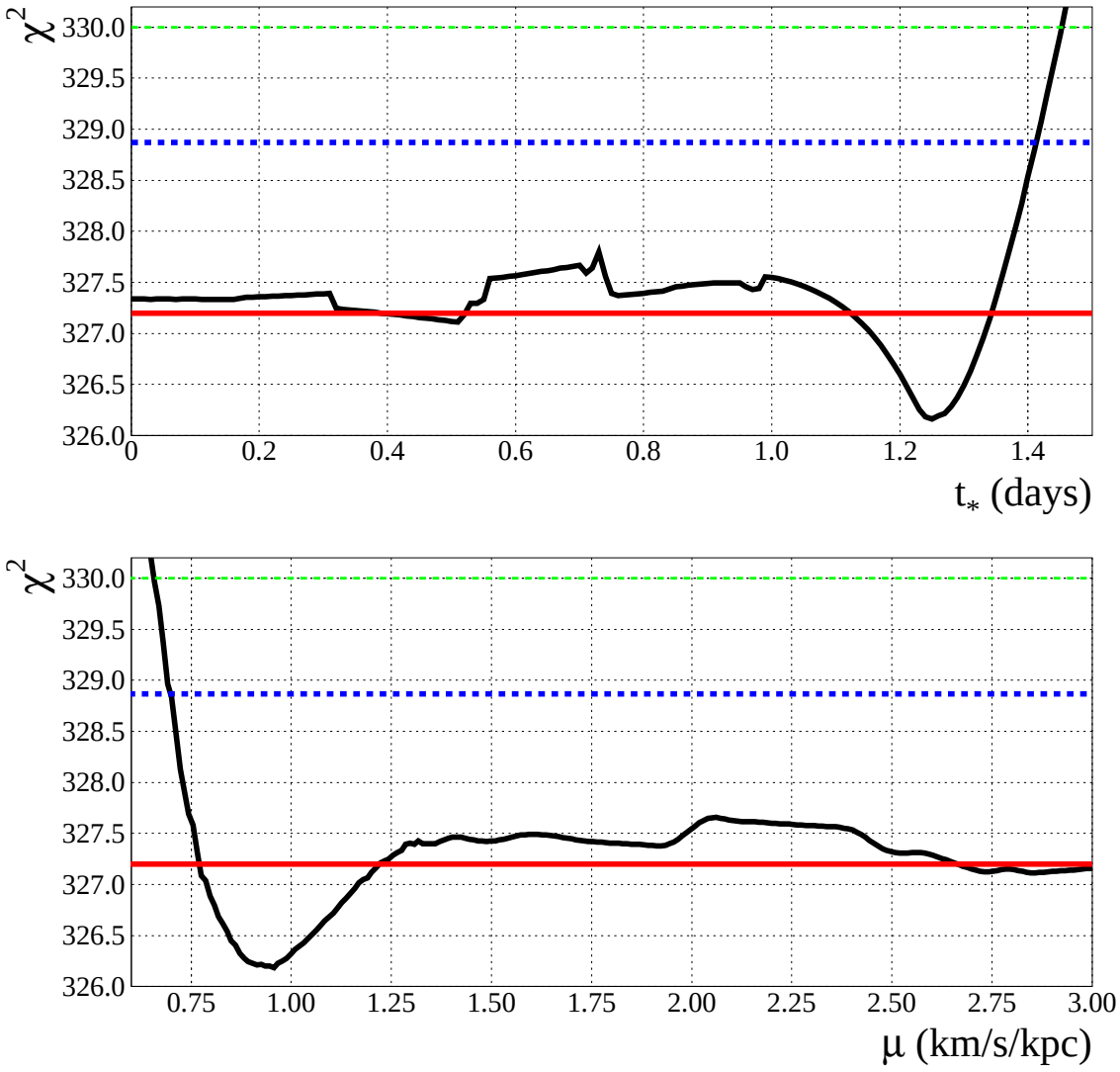

FIG. 3.— Plots of χ^2 vs the source radius crossing time (t_*, top panel) and χ^2 vs the lens proper motion (μ). Bottom panel: we use an estimate of the source angular radius of 0.67 μas (Sect. 2.2). The solid, dashed and thin dashed lines indicate the 68.3%, 90% and 95% confidence level, respectively.

of our results on μ we finally recall the useful relationship

$$\theta_* = a\sqrt{\phi}\,, \tag{4}$$

where the coefficient a depends only on the color (ϕ is the source flux). In particular this allows us to carry out the χ^2 analysis (Fig. 3, bottom panel), in the 3-d parameter space $t_{\rm E}$, ρ and ϕ.

The value for the lens proper motion we obtain, corresponding to the best fit value, is $\mu = 0.93\,{\rm km\,s^{-1}\,kpc^{-1}}$. The discussed large residual degeneracy for the angular radius ρ, and the related aspects discussed above, lead us however to report, as a more robust outcome of the present analysis, an *upper* limit for ρ (and t_*) and a *lower* limit for μ only. At 68.3% level we get

$$\begin{aligned} \rho &< 0.22\,, \\ t_* &< 1.35 \quad \text{days}\,, \\ \mu &> 0.75 \quad {\rm km\,s^{-1}\,kpc^{-1}}\,. \end{aligned}$$

For the lens proper motion we also get $\mu > 0.68\,(0.64)$ ${\rm km\,s^{-1}\,kpc^{-1}}$ at the 90% (95%) level, respectively.

3. DISCUSSION

The results of the light curve analysis presented in Sect. 2.2, that in particular confirm the outcome on the source magnitude discussed in Sect. 2.1, can be used to establish the lens nature of the OAB-N2 event. As previously discussed, the relevant issue is to distinguish between self lensing and MACHO lensing. To this end we focus on the lens-source relative proper motion, μ, because it is independent of the lens mass and so depends only on the kinematics

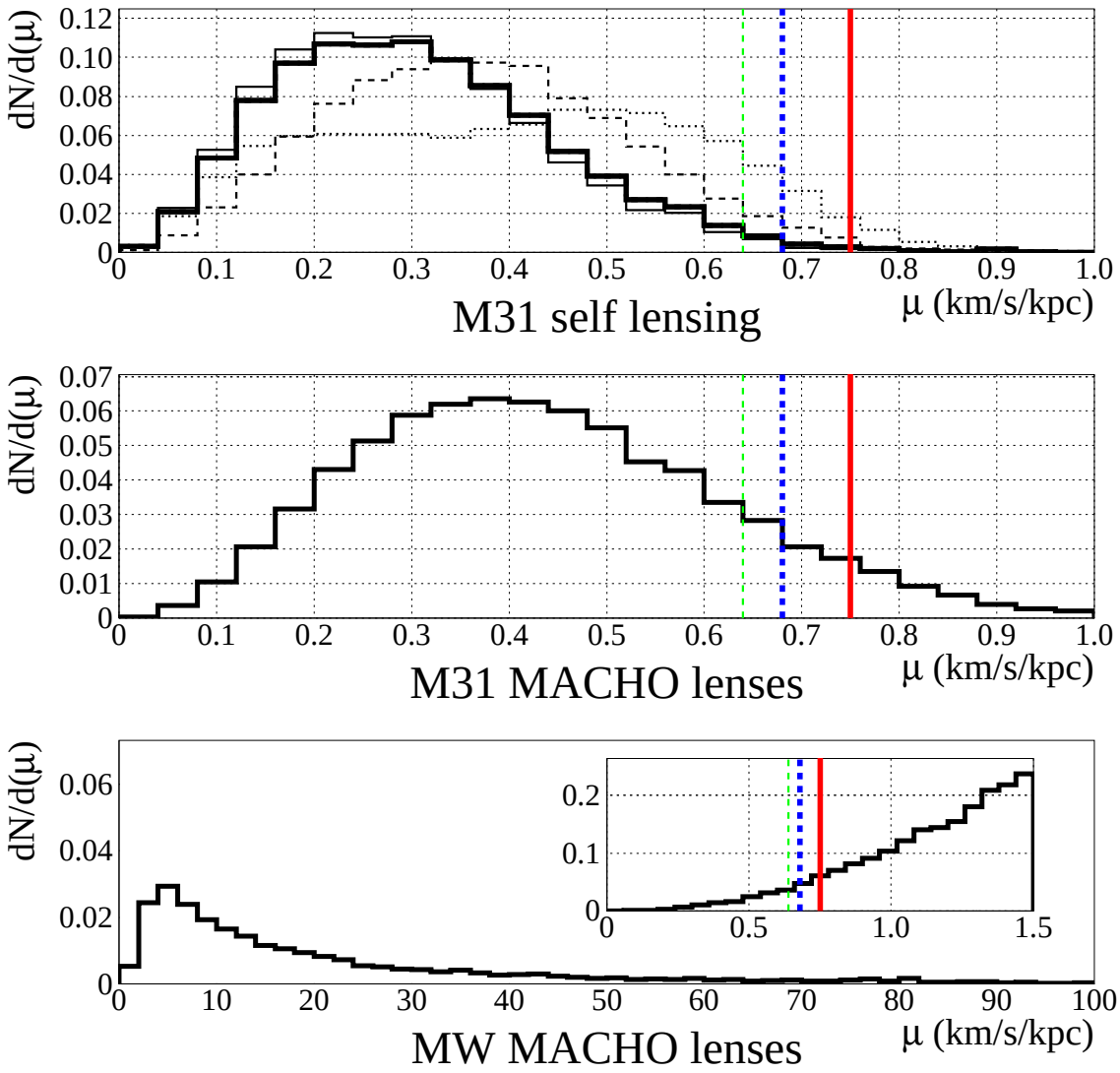

FIG. 4.— Expected distributions for the lens proper motion, μ, along the line of sight toward the OAB N2 position for different source-lens populations evaluated within the Monte Carlo simulation of the experiment. Top panel: thin solid, dashed and dotted lines are for bulge sources and bulge and disc lenses and disc-disc events, respectively; thick solid line for the overall M31 self lensing (each distribution is normalized to 1 separately). Bulge-bulge events are expected to contribute for about 80% of the expected signal; MW disc events (not shown, for which the lens proper motion distribution is expected to peak well beyond 1 $\mathrm{km\,s^{-1}\,kpc^{-1}}$) are expected to be negligibile (see text for details). Middle (bottom) panels: M31 (MW) MACHO lenses with the overall (M31+MW) MACHO distributions normalized to 1, and 75% signal expected from M31 lenses (in the inset, bottom panel, showing a zoom for the MW MACHO distribution, the units are 10^{-3}). The solid, dashed and thin dashed vertical lines (68.3%, 90% and 95% level, respectively) indicate the *lower* limit for the lens proper motion derived in the light curve analysis (Sect. 2.2, Fig. 3).

and spatial distribution of the lens population. The potential role played by the lens proper motion, also in relation to M31 pixel lensing, has been first discussed in Gould (1994); Han & Gould (1996). In these analyses the emphasis was given in particular to the possibility to constrain MW MACHO lenses with respect to M31 lenses. This is relevant as MW MACHOs are expected to contribute, for given MACHO mass and mass halo fraction, for about one third of the overall expected MACHO signal. The identification of MW lenses would therefore give a strong indication for a MACHO signal. In the following we will point out how and to which extent an analysis of the lens proper motion may allow one to distinguish also between the different M31 lens populations.

As a tool of analysis, to compare with the outcome of the light curve fit, we will make use of the Monte Carlo simulation of the experiment described in Calchi Novati et al. (2009a). As a prior we consider the line of sight toward the OAB-N2 position (this gives however only marginal quantitative differences from the more general case in which the overall PLAN field of view is considered). We also recall that as an output we have only light curves that are *selected* within the Monte Carlo (where in particular the experimental set up is carefully reproduced together with a basic selection pipeline).

At the OAB-N2 position, only $\approx 3'$ from the M31 center, the dominant contribution from M31 self lensing is expected from events with bulge sources and bulge lenses. Specifically, we expect $\sim 80\%$ of events to belong to these populations, with the rest equally divided between bulge-disc (both source-lens and lens-source) events, with only a

marginal 1% of disc-disc events. In Fig. 4 we present the results of the Monte Carlo simulation for the lens proper motion distributions for different source and lens populations. The most striking outcome for our purposes is the threshold at about $\mu_{\rm th} \sim 1$ km s^{-1} kpc^{-1}, such that for $\mu > \mu_{\rm th}$ we expect almost no M31 lens events, while on the other hand almost all of MW lens events are expected to fall in this region. This is easily explained on the basis that finite size effect is never important for MW events (for which on average the Einstein angular radius, proportional to the square root of the lens-source distance over the lens distance, is about one hundred times larger than for M31 events and $\rho \propto \theta_{\rm E}^{-1}$) and for which, on the other hand, the lens distance is by far smaller. The relatively large lower limit value we find for the lens proper motion might therefore be taken as an indication for the lens to belong to the MW halo. (This outcome, however, would be clearly at odd with the discussed marginal indication we find for finite size source effect.) However large, the lower limit for the lens proper motion is still fully compatible with M31 lensing. In particular, among M31 lensing events, we find that a broader distribution for μ is expected for MACHO lensing, while the limit we find is hardly compatible with the expected distribution for bulge-bulge events. Although we can not certainly rule out, for this specific event, the self-lensing hypothesis, this outcome strongly suggests the MACHO lensing hypothesis for the OAB-N2 event.

More specifically, corresponding to the 68.3% lower threshold obtained above, $\mu > 0.75$ km s^{-1} kpc^{-1}, for M31 MACHO lensing we still have about (for bulge source events and similarly for disc source events that represent, however, only about 15% of the expected M31 MACHO signal) 6% of the expected signal (10% and 14% respectively at the 90% and 95% levels). On the other hand, at the 68.3% level, we expect less than 1% of the overall bulge-bulge signal (still about 70% of the overall M31 self lensing signal) and about 1% of bulge-disc and disc-bulge lenses. At 95% level these ratio rise to almost 2% for bulge-bulge events (about 60% of the overall M31 self lensing signal) and to almost 5% for bulge-disc and disc-bulge lenses. Although in an absolute sense M31 disc-disc events give only a marginal contribution, it is worth noticing that, along this M31 central line of sight, they show a marked bimodal distribution for the lens proper motion with a long tail for large values of μ. In particular, larger than the 68.3%, 90% and 95% threshold values we still find, respectively, 2.6%, 7.2% and 12% of the expected events belonging to this population. Overall, at the 68.3%, 90% and 95% levels, we expect respectively about 0.6%, 1.3% and 2.1% of the M31 self-lensing signal.

Besides M31 bulge and disc lenses, in principle one might consider also *Galactic* disc lenses. Using standard models for the MW disc (Han & Gould 2003; Calchi Novati et al. 2008) the ratio of the expected number of events for this population is below 1% with respect to M31 self lensing[10]. This result, joined to the overall outcome of one, possibly two, microlensing events reported from the 2007 PLAN campaign (Calchi Novati et al. 2009a) makes the possibility for OAB-N2 to be a MW disc event extremely unlikely. However, for MW lensing, the lens proper motion is much larger than for M31 lensing and this applies even more strongly to stellar lensing than MACHO lensing for these two galaxies. In fact, typical values are well above 1 km s^{-1} kpc^{-1}, larger, on average, than for MW MACHOs. Hence, in particular almost *all* of the expected MW disc events fulfill the lower limit condition we find on the lens proper motion. Larger than the 95% level lower limit, the even small fraction of expected M31 self lensing events is however still larger than the overall expected MW disc signal. The overall small number of expected MW disc events makes therefore this contribution always negligible (so that in particular we do not show it in Fig. 4).

As for the Einstein time scale, which is rather well constrained from the light curve fit, comparing to the Monte Carlo distributions we find the fit result to match the expected self-lensing signal characteristics well. For MACHO lensing the result is dependent on the lens mass. The fit result is fully compatible with MACHO in the mass range $(10^{-2} - 10^{-1})$ M$_\odot$, but still compatible with even larger MACHO mass as 0.5 M$_\odot$.

Finally, we comment on our result for the finite source size effect, with the best fit value indicating a signature for $\rho > 0$. As already pointed out this effect is expected for M31 lenses only. Still, the value we find (as reflected also in the proper motion best fit value) has an a priori low probability. Together with the only marginal detection, with a $\Delta\chi^2 \sim 1$ to separate from the case with no finite size effect, this makes this detection only "possible".

4. CONCLUSION

In the present paper we have presented an updated analysis of the M31 microlensing candidate event OAB-N2 first reported by the PLAN collaboration in Calchi Novati et al. (2009a). In this previous work, in particular, the insufficient sampling along the flux variation did not allow us to probe unambiguously the microlensing nature of this flux variation. Here we have taken advantage of newly available WeCAPP data to complete the light curve sampling. From a methodological perspective, we observe that the importance of merging different data sets for microlensing observation might look even trivial when considering that Galactic Bulge events are routinely observed by multiple telescopes when searching for planetary anomalies. The present analysis, however, shows the extent to which this is suitable, feasible and, as this case nicely shows, possibly essential also for M31 pixel lensing events. (Such a strategy, besides, is unavoidable in order to achieve the challenging purpose of a systematic research for exoplanets in M31, Covone et al. 2000; Baltz & Gondolo 2001; Chung et al. 2006; Ingrosso et al. 2009. A first attempt in this sense is being carried out by the ANGRSTOM collaboration Kerins et al. 2006; Darnley et al. 2007; Kim et al. 2007. The usually short expected timescale, $t_{\rm FWHM}$, makes however potentially important such a strategy also for "normal" single-lens events.).

A preliminary analysis on archival images of the 4m Mayall-KPNO telescope and of WFPC2/HST allowed us to

[10] Furthermore, a sizeable fraction of these MW events is expected, because of the extremely small observer-lens distance, to have too bright lenses for being suitable candidates.

reject the tentative identification of the OAB-N2 source made in Calchi Novati et al. (2009a) with a rather bright Massey et al. (2006) M31 catalog source. The event source, in fact, appears to be a nearby fainter blended object on the KPNO image, as confirmed also by the HST analysis. Although we can not conclusively determine the source magnitude, because of blending and the huge background level, even this partial result is a first step toward a better characterization of this event. Indeed, the new light curve photometry analysis confirms that the source must be a fainter object than previously concluded.

The improved sampling along the OAB-N2 light curve then allows us to reach a few important conclusions. First, we find a strong confirmation of the microlensing nature of this flux variation. The flux variation characteristics, the large signal to noise ratio, the short duration and the position, within the inner $3'$ of M31 where the expected rate is larger, together with the further evidence provided by the joint analysis of two completely independent data sets, put this flux variation among the most convincing and interesting M31 microlensing events reported so far. Second, we have carried out a more detailed analysis in the event microlensing parameter space with the specific purpose to constrain the lens nature, whether due to self lensing or to MACHO lensing. The main outcome we get to is a *lower* limit for the relative source-lens proper motion, μ. As we have shown, this parameter, independent of the lens mass and therefore less subject to model issues, not only may allow one to distinguish M31 lensing from MW lensing (where the main expected signal is MACHO lensing and for which μ is significantly larger than for M31 lensing) but also among different M31 lens populations. Specifically, at 95% level, we find $\mu > 0.64\ \mathrm{km\,s^{-1}\,kpc^{-1}}$. Comparing to the output of the Monte Carlo simulation of the experiment we conclude that, if not to the MW halo population, this value is more compatible with M31 MACHO lensing rather than with self lensing, for which only about 2% of the overall population is expected to fulfill this constraint. Although the self lensing hypothesis can not be definitively ruled out for this single specific event so that we are not yet in a position to strongly discriminate self lensing from MACHO lensing, this analysis shows the extent to which the lens proper motion, with no other prior assumptions on MACHOs but their spatial distribution and kinematics, is a powerful tool toward this purpose.

As an intermediate step of the light curve fit χ^2-based analysis we have looked for possible signatures of finite size source effect (through a study of the normalized angular radius, ρ) for which however we find only marginal indications. We recall that an evidence in this sense would imply that the lens belongs to some M31 populations. The robust outcome we get to is rather an *upper* limit for ρ and on the related quantity, the source radius crossing time, $t_* = \rho\, t_{\rm E}$ which, together with an estimate, from the source magnitude and color, of the physical angular radius, finally gives us the aforementioned *lower* limit for the lens proper motion.

The outcome of this analysis is affected by the lack of an accurate and precise estimate of the unresolved source magnitude and color, independent of the light curve fit, for which a focused proposal on HST data would be extremely welcomed.

In the framework of M31 pixel lensing, the present analysis of OAB-N2 is the third example, following those for the events PA-N1 (Aurière et al. 2001) and PA-S3/GL1 (Riffeser et al. 2008), where a detailed investigation of the lensing parameter space allowed to draw conclusions on the lens nature. Interestingly, although in the present work with a worse confidence level with respect to that reported in Riffeser et al. (2008) for PA-S3/GL1 and with the caveats discussed in the Introduction as for PA-N1, in all cases the analyses point toward the same outcome, namely that MACHO lensing should be preferred over self lensing.

We warmly acknowledge the WeCAPP collaboration, in particular A. Riffeser and S. Seitz, for making available to us, prior to their publication, the WeCAPP data relative to the OAB-N2 light curve. SCN, VB, LM and GS acknowledge support by MIUR through PRIN Prot. 2008NR3EBK_002, and by FARB of the Salerno University.

REFERENCES

Alard, C., & Lupton, R. H. 1998, ApJ, 503, 325
Alcock, C., et al. 2000, ApJ, 542, 281
Ansari, R., et al. 1997, A&A, 324, 843
Aurière, M., et al. 2001, ApJ, 553, L137
Baillon, P., Bouquet, A., Giraud-Heraud, Y., & Kaplan, J. 1993, A&A, 277, 1
Baltz, E. A., & Gondolo, P. 2001, ApJ, 559, 41
Baltz, E. A., & Silk, J. 2000, ApJ, 530, 578
Belokurov, V., et al. 2005, MNRAS, 357, 17
Bennett, D. P. 2005, ApJ, 633, 906
Calchi Novati, S. 2009, arXiv:0912.2667, to be published in GRG
Calchi Novati, S., et al. 2009a, ApJ, 695, 442
Calchi Novati, S., et al. 2007, A&A, 469, 115
Calchi Novati, S., de Luca, F., Jetzer, P., Mancini, L., & Scarpetta, G. 2008, A&A, 480, 723
Calchi Novati, S., De Luca, F., Jetzer, P., & Scarpetta, G. 2006, A&A, 459, 407
Calchi Novati, S., et al. 2002, A&A, 381, 848
Calchi Novati, S., Mancini, L., Scarpetta, G., & Wyrzykowski, Ł. 2009b, MNRAS, 400, 1625
Calchi Novati, S., et al. 2005, A&A, 443, 911
Chung, S.-J., et al. 2006, ApJ, 650, 432
Claret, A. 2000, A&A, 363, 1081
Covone, G., de Ritis, R., Dominik, M., & Marino, A. A. 2000, A&A, 357, 816
Crotts, A. P. S. 1992, ApJ, 399, L43
Cseresnjes, P., Crotts, A. P. S., de Jong, J. T. A., Bergier, A., Baltz, E. A., Gyuk, G., Kuijken, K., & Widrow, L. M. 2005, ApJ, 633, L105
Darnley, M. J., et al. 2007, ApJ, 661, L45
de Jong, J. T. A., et al. 2006, A&A, 446, 855
Dolphin, A. E. 2000, PASP, 112, 1383
Dominik, M. 2009, MNRAS, 393, 816
Dominik, M. 2010, doi:10.1007/s10714-010-0930-7, to be published in GRG
Gaudi, B. S. 2010, arXiv:1002.0332
Gondolo, P. 1999, ApJ, 510, L29
Gössl, C. A., & Riffeser, A. 2002, A&A, 381, 1095
Gould, A. 1994, ApJ, 421, L71
Gould, A. 1995, ApJ, 441, 77
Gould, A. 1996, ApJ, 470, 201
Gyuk, G., Dalal, N., & Griest, K. 2000, ApJ, 535, 90
Han, C., & Gould, A. 1996, ApJ, 467, 540
Han, C., & Gould, A. 2003, ApJ, 592, 172
Ingrosso, G., Calchi Novati, S., de Paolis, F., Jetzer, P., Nucita, A. A., Scarpetta, G., & Strafella, F. 2007, A&A, 462, 895

Ingrosso, G., Calchi Novati, S., de Paolis, F., Jetzer, P., Nucita, A. A., & Strafella, F. 2006, A&A, 445, 375
Ingrosso, G., Novati, S. C., de Paolis, F., Jetzer, P., Nucita, A. A., & Zakharov, A. F. 2009, MNRAS, 399, 219
Jetzer, P. 1994, A&A, 286, 426
Kerins, E., Darnley, M. J., Duke, J. P., Gould, A., Han, C., Jeon, Y.-B., Newsam, A., & Park, B.-G. 2006, MNRAS, 365, 1099
Kerins, E., Darnley, M. J., Duke, J. P., Gould, A., Han, C., Newsam, A., Park, B., & Street, R. 2010, arXiv:1004.2166, submitted to MNRAS
Kervella, P., Bersier, D., Mourard, D., Nardetto, N., Fouqué, P., & Coudé du Foresto, V. 2004, A&A, 428, 587
Kim, D., et al. 2007, ApJ, 666, 236
Lee, C., Riffeser, A., Seitz, S., & Bender, R. 2009, ApJ, 695, 200
Mancini, L., Calchi Novati, S., Jetzer, P., & Scarpetta, G. 2004, A&A, 427, 61
Marigo, P., Girardi, L., Bressan, A., Groenewegen, M. A. T., Silva, L., & Granato, G. L. 2008, A&A, 482, 883
Massey, P., Olsen, K. A. G., Hodge, P. W., Strong, S. B., Jacoby, G. H., Schlingman, W., & Smith, R. C. 2006, AJ, 131, 2478
Massey, R., Kitching, T., & Richard, J. 2010, arXiv:1001.1739, submitted to Rep.Prog.Phys
Monet, D. G., et al. 2003, AJ, 125, 984
Moniez, M. 2010, arXiv:1001.2707, to be published in GRG
Paczyński, B. 1986, ApJ, 304, 1
Paulin-Henriksson, S., et al. 2003, A&A, 405, 15
Riffeser, A., Fliri, J., Bender, R., Seitz, S., & Gössl, C. A. 2003, ApJ, 599, L17
Riffeser, A., et al. 2001, A&A, 379, 362
Riffeser, A., Fliri, J., Seitz, S., & Bender, R. 2006, ApJS, 163, 225
Riffeser, A., Seitz, S., & Bender, R. 2008, ApJ, 684, 1093
Sahu, K. C. 1994, Nature, 370, 275
Schlegel, D. J., Finkbeiner, D. P., & Davis, M. 1998, ApJ, 500, 525
Tisserand, P., et al. 2007, A&A, 469, 387
van Belle, G. T. 1999, PASP, 111, 1515
van Hamme, W. 1993, AJ, 106, 2096
Witt, H. J., & Mao, S. 1994, ApJ, 430, 505
Wozniak, P., & Paczynski, B. 1997, ApJ, 487, 55
Wyrzykowski, Ł., et al. 2009, MNRAS, 397, 1228
Yoo, J., et al. 2004, ApJ, 603, 139